Journal of Power Sources 228 (2013) 32–38

Contents lists available at SciVerse ScienceDirect

Journal of Power Sources

journal homepage: www.elsevier.com/locate/jpowsour

Effects of nonaqueous electrolyte solutions mixed with carbonate-modified siloxane on charge–discharge performance of negative electrodes for secondary lithium batteries

Yasuhiro Takei [a], Kazuhiko Takeno [b], Hideyuki Morimoto [a], Shin-ichi Tobishima [a,*]

[a] Department of Chemistry, Faculty of Engineering, Gunma University, Kiryu, Gunma 376-8515, Japan
[b] NTT Docomo, Inc., R&D Center, 3-6 Hikarino-oka, Yokosukas-shi, Kanagawa 239-8536, Japan

HIGHLIGHTS

- Carbonate modified siloxane mixed with 1 M $LiPF_6$-EC/EMC are prepared.
- Cycling efficiencies of Li, Si–SiO_2–carbon composite and Fe_2O_3 anodes are improved.
- Siloxane suppresses excess reduction of $LiPF_6$-EC/EMC by lithium.
- Model of interface between anode and electrolyte is proposed.

ARTICLE INFO

Article history:
Received 27 September 2012
Received in revised form
21 November 2012
Accepted 24 November 2012
Available online 29 November 2012

Keywords:
Lithium cell
Electrolyte
Rechargeable cell
Siloxane
Cell safety
Cycling efficiency

ABSTRACT

Influence of mixing carbonate-modified siloxane into 1 M (M: mol L^{-1}) $LiPF_6$-ethylene carbonate (EC)/ethylmethyl carbonate (EMC) (mixing volume ratio = 3:7) mixed solvent electrolytes on charge–discharge cycling properties of lithium is examined. As siloxane, 4-(2-bis(trimethylsilyloxy)methylsilylethyl)-1,3-dioxolan-2-one is investigated. Charge–discharge cycling efficiencies of lithium metal anodes are improved and impedance of anode/electrolyte interface decreases by mixing siloxane, compared with those in 1 M $LiPF_6$-EC/EMC alone. Mechanism of enhancement of lithium cycling efficiency is considered to be due to the suppression of excess reduction of $LiPF_6$-EC/EMC by lithium and growth of surface film (SEI, solid electrolyte interphase) on lithium. Infrared study indicates that SEI formed in $LiPF_6$-EC/EMC with siloxane contains more inorganic compounds than that in $LiPF_6$-EC/EMC alone. Better cycling behavior of α-Fe_2O_3 and Si–SiO_2–carbon composite anodes is obtained by mixing siloxane. Thermal behavior of electrolyte solutions toward graphite-lithium anodes is evaluated with a differential scanning calorimeter. Heat-output of graphite–lithium anodes with 1 M $LiPF_6$-EC/EMC electrolyte solutions tends to decrease by mixing siloxane.

1. Introduction

Many of commercial lithium ion cells are composed of carbon anode and $LiCoO_2$ cathode with nonaqueous electrolyte solutions. Typical example of nonaqueous electrolyte solutions is $LiPF_6$-ethylene carbonate (EC)/ethylmethyl carbonate (EMC). The improvement of energy density of lithium ion cells has been required every year. However, now the capacity of carbon anodes is getting closer to the theoretical value (372 mAh g^{-1}). Then, new anode materials exhibiting higher energy density than carbon have been studied. Examples of these materials are lithium metal, various Si-based and Sn-based compounds [1]. In addition, Li/air(O_2) and Li/S cells have been studied as next generation lithium ion cells. These cells use lithium or lithium alloy anodes since original cathodes do not have lithium. However, at this stage, cycleability of these materials is not sufficient for commercial use. The choice of electrolyte materials (solvents, solutes and additives) is one of the most important factors for charge–discharge cycling performance of lithium cells with various anodes.

Many researches on the electrolyte solutions have been carried out for improving lithium cycleability [2]. One of these researches is to modify and stabilize the chemical structure of carbonate solvents by introducing fluorine atoms. Examples of these solvents are fluoro-cyclic carbonates such as fluoro-EC, fluoro-propylene carbonate and fluoro-linear carbonates such as fluoro-methylacetae, fluoro-ethyl-emethyl carbonate, fluoro-diethyl carbonate, and fluoro-dimethyl

* Corresponding author. Tel.: +81 277 30 1382; fax: +81 277 30 1380.
E-mail address: stobishima@gunma-u.ac.jp (S.-i. Tobishima).

0378-7753/$ – see front matter © 2012 Elsevier B.V. All rights reserved.
http://dx.doi.org/10.1016/j.jpowsour.2012.11.096

carbonate [3–5]. Also, various additives for electrolyte solutions have been studied. Typical example is vinylne carbonate (VC). VC has high reduction potential and forms a good surface film on anodes such as lithium metals and carbons for the improvement of cycling efficiency [6]. Also, organosilicon compounds such as dimethylsilan [7] and EC with Si-contained side-chains [8] have been investigated. These organosilicon compounds exhibit similar behavior as VC does. These silans are reactive toward lithium and produce a good surface film on lithium for enhancing stability of lithium anodes [7].

In our previous works, influence of organic silicon compounds as electrolyte additives to $LiPF_6$-EC/EMC on lithium cycling efficiency has been reported [9,10]. As organic silicon compounds, poly-ether modified siloxanes [9] and carbonate modified siloxanes [10] were examined. Chemical bonding of Si–O is stronger and more stable than that of C–O. These siloxanes are colorless and clear liquid at room temperature. Lithium cycling efficiencies were improved by mixing these siloxanes. These compounds are less reactive toward lithium than $LiPF_6$-EC/EMC and adsorbed on the lithium anode surface. This adsorption layer suppresses the lithium dendrite formation and the reduction of electrolyte solutions by lithium [10]. This mechanism is similar to an addition of surfactants (surface active agents) to electrolyte solutions such as polyethyleneglycol dimethyl ethers [11]. Among carbonate modified siloxanes examined in previous work, 4-(2-bis(trimethylsilyloxy) methylsilylethyl)-1,3-dioxolan-2-one exhibited best lithium cycling efficiency. In this paper, this siloxane is called as sample B. Fig. 1 shows chemical structure of sample B. However, there is a problem to be dissolved. When carbonate modified siloxanes were examined in previous work [10], siloxanes were simply mixed with 1 M $LiPF_6$-EC/EMC (3:7 in volume ratio). Then, concentration of $LiPF_6$ in prepared electrolyte solutions decreased by mixing siloxane. Cycling efficiencies of lithium depended on siloxane amounts and showed maximum efficiencies around high siloxane amount of 60 vol.%. So, further investigation must be necessary for electrolyte solutions with constant concentration of $LiPF_6$ to clarify effects of carbonate modified siloxanes on cycleability of lithium. Also, thermal stability of electrolyte solutions is affected by solute concentration.

In this work, we examine influence of carbonate-modified siloxane as co-solvent of EC/EMC (3:7 in volume mixing ratio) mixed solvent electrolytes keeping constant concentration of 1 M (M: mol L^{-1}) $LiPF_6$ on lithium cycling efficiency. As a carbonate modified siloxane, 4-(2-bis(trimethylsilyloxy)methylsilylethyl)-1,3-dioxolan-2-one (sample B) is investigated. Mechanism for change in lithium cycling efficiency by mixing siloxane is discussed by investigating properties of interface between lithium and electrolyte solutions by ac impedance and infrared spectroscopy. In addition, influence of carbonate modified siloxane on other anode materials than lithium metal (Si-based compounds and α-Fe_2O_3), is also examined here. These anode materials are charged to close to 0 V vs. Li/Li+. So, as in case of lithium metal, suppression of electrolyte reduction by lithium is necessary to improve charge–discharge cycling efficiencies.

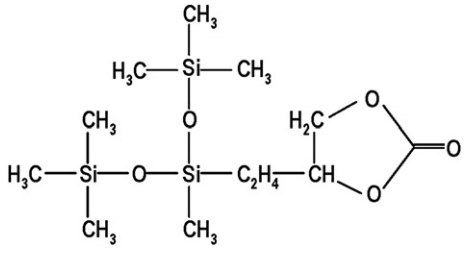

Fig. 1. Chemical structure of carbonate-modified siloxane, sample B: 4-(2-bis (trimethylsilyloxy) methylsilylethyl)-1,3-dioxolan-2-one.

2. Experimental

2.1. Preparation of electrolyte solutions

Siloxane was obtained from Shin-Etsu Chemical Corporation. Electrolyte solutions were prepared by mixing siloxane, $LiPF_6$ and EC/EMC (3:7 in volume ratio) (Tomiyama Pure Chemicals Co., Lithium Battery Grade). Mixing ratio of EC/EMC was fixed as 3:7 in volume ratio. Concentration of $LiPF_6$ was fixed as 1 M for all ternary mixed solvent of [EC/EMC (3:7) + siloxane]. Hereafter, "EM" represents 1 M $LiPF_6$-EC/EMC (3:7) and "EM + sample B (60 vol.%)" represents 1 M $LiPF_6$-[EC/MEC (3:7)(40 vol.%) + sample B (60 vol.%)]. Sample B can be mixed with 1 M $LiPF_6$-EC/EMC (3:7) up to 95 vol.%.

2.2. Charge–discharge cycling tests of various anodes

Charge–discharge cycling tests of lithium metal were carried out galvanostatically, using a coin cell (coin type 2032, diameter 20 mm in diameter, 3.2 mm in thickness) with a lithium metal sheet counter electrode (0.1 mm thickness, 15 mm diameter) and a stainless steel (SUS 316) cathode case of the coin cell as the working electrode. SUS stands for steel use stainless steel. SUS 316 is very stable among various SUSs and contains 18%Cr, 12%Ni and 2.5%Mo. In charge–discharge voltage curves, charge–discharge behavior of other metals than Li is not observed. The charge–discharge cycling efficiency (Eff) was obtained from the ratio of the stripping charge (Qs)/plating charge (Qp) on the stainless steel electrode. Plating Li on SUS was carried out every cycle at a charge current density of 0.5 mA cm^{-2} for 1 h. The Qp had a constant value of 0.50 mAh cm^{-2}. Stripping of Li^+ ions (discharge) from Li deposited on SUS was carried out at a charge current density of 0.5 mA cm^{-2}. 1.5 V was used as an end point of stripping [9,10]. The charge–discharge current density was defined as Ips.

In cases of natural graphite electrodes, the charge–discharge tests were carried out by the charge–discharge voltage cut-off (0.005 and 1.5 V vs. Li/Li^+) with a constant current density of 0.5 mA cm^{-2} by using the 2032 coin Li/graphite cells. In cases of Si–SiO_2–carbon composite (Si–C) and α-Fe_2O_3 electrodes, the charge–discharge tests were carried out by the charge–discharge voltage cut-off (0 and 2.0 V vs. Li/Li^+) and (0.005 and 3.0 V vs. Li/Li^+), respectively, with a constant current density of 0.5 mA cm^{-2} at first cycle and 0.2 mA cm^{-2} at cycles after second cycle by using the 2032 coin Li/Si–C and Li/α-Fe_2O_3 cells. These cells have a lithium metal counter electrode and the working electrode of graphite, Si–C or α-Fe_2O_3.

For coin cell fabrications, we prepared the printed electrodes as working electrodes. The printed carbon electrodes were prepared by coating a Ni sheet with a mixture of carbon powder (around 18 mg) and poly (vinylidene fluoride) (PVDF) (weight ratio of carbon:PVDF = 9:1) in N-methyl pyrolidinone (NMP). We then evacuated the solvent and dried the electrodes. The printed carbon electrodes are 15 mm in diameter and 0.15 mm in thickness. Natural graphite powder used here has an average particle size of 10.7 μm in diameter, a surface area of 10.3×10^3 m kg^{-1} and a density of 0.21 kg m^{-3}.

The printed Si–C electrodes (15 mm in diameter and 0.15 mm in thickness) were prepared by similar method as natural graphite electrodes by using Si–C powder and polymer binder. Si–C material was prepared according to the papers [12–14] by methane–argon gas mixture-chemical vapor deposition (CVD) with 1100 °C heat treatment. Image of this final product of Si–C material is

shown in Fig. 2. Fine silicon crystal was distributed in the SiO_2. The surface of the final product was covered with double layers composed of thin inside layer of SiC (silicon carbide) and thick outside layer of carbon.

The printed α-Fe_2O_3 electrodes (15 mm in diameter and 0.15 mm in thickness) were prepared by similar method as natural graphite electrodes by using α-Fe_2O_3 powder and polymer binder [15].

All the electrochemical measurements were carried out at 25 °C.

2.3. Thermal stability tests of electrolyte solutions

Thermal behavior of the electrolyte solutions toward C_6Li_x (C: natural graphite) was evaluated with a differential scanning calorimeter (DSC, Rigaku Co., model TAS-100) and a crimp-sealed stainless steel pan. In the thermal stability tests of the electrolyte solutions toward C_6Li_x, the DSC sample was composed of about 7 mg of carbon and 3 μl of electrolyte. All the DSC experiments were carried out at a heating rate of 10 °C min^{-1} from room temperature to 450 °C. As described in Section 2.2, C_6Li_x was prepared by charge–discharge of the Li/natural graphite coin cells.

2.4. AC impedance and conductivity measurements

The AC impedance measurements of lithium/electrolyte interface were carried out using Li/SUS coin cells with an impedance analyzer (Iviumstat, Hokuto Denko Co.). AC frequency range was 100 MHz–20 kHz and amplitude of vibration was 20 mV. Conductivity of electrolyte solutions was measured using symmetry cell with platinum black electrodes at 1 kHz AC impedance.

2.5. Infrared spectroscopy

Fourier transform-Infrared (FT-IR) spectroscopy was carried out to investigate chemical composition of surface film on anodes (IRAffinity-1, Shimadzu Corporation). Experimental procedure is described in Section 3.1.

3. Results and discussion

3.1. Electrolyte conductivity

Fig. 3 shows relationship between electrolyte conductivity, mixing volume ratio of siloxane (sample B) and temperature for 1 M $LiPF_6$-[EC/EMC (30:70 in volume ratio) + siloxane] ternary mixed solvent electrolytes. With an increase in siloxane content, conductivity tended to decrease. At 20 °C, EM showed conductivity of 8.9 mS cm^{-1} while EM + sample B (20 vol.%) showed 5.3 mS cm^{-1} and EM + sample B (60 vol.%) showed 1.5 mS cm^{-1}. Viscosity (ion migration speed) affects conductivity more strongly than dielectric constant (degree of ionic dissociation) in many cases of $LiPF_6$-organic solvents such as $LiPF_6$-EC/EMC [16]. With an increase in siloxane content, viscosity increases since siloxane has

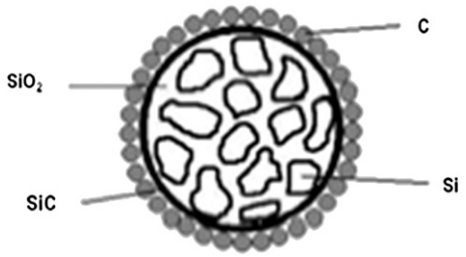

Fig. 2. Image of Si–SiO_2–carbon composite (Si-C).

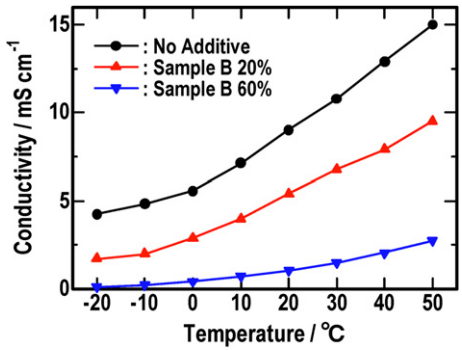

Fig. 3. Conductivity of 1 M $LiPF_6$- [EC/MEC (30:70 vol.%) + siloxane (sample B)].

higher viscosity (22.5 × 10^{-3} N m^{-2} at 20 °C) than that of EC/EMC (30:70 in volume ratio) (1.18 × 10^{-3} N m^{-2}) [10]. With an increase in temperature, conductivity increases. This phenomenon also arises from influence of the viscosity since both viscosity and dielectric constant increase with a reduction in temperature [17].

3.2. Charge–discharge cycling properties of lithium metal anodes in the electrolyte solutions with siloxane

Charge–discharge cycling tests of lithium in EM + siloxane were carried out by using coin cells consisted of Li anode and SUS cathode. Fig. 4 shows relation between charge–discharge cycling efficiencies of lithium and cycle number in EM with and without siloxane. Fig. 5 show average lithium cycling efficiencies from first to 10th cycle ($Eff_{Ave.\ 10}$), to 20th cycle ($Eff_{Ave.\ 20}$) and to 30th cycle ($Eff_{Ave.\ 30}$) in EM + siloxane. Average efficiencies in EM + siloxanes were higher than that in EM alone. Average efficiencies exhibited the maximum value at 60 vol.% sample B. From the charge–discharge test results, it was found that the addition of siloxane was effective for the improvement of cycling efficiency of lithium metal anodes.

3.3. AC impedance measurement results for interface between lithium electrode and electrolyte solutions

In organic electrolyte solutions, surface of lithium is covered with thin film after charge–discharge cycling [18]. This surface film is formed by reduction of electrolyte solution by lithium. This film is generally known as SEI (solid electrolyte interphase) [19]. SEI is consisted of several organic and inorganic compounds such as lithium alkyl carbonate and Li_2CO_3 [18]. During charge and discharge, lithium ion must diffuse in SEI. Not only charge transfer but also

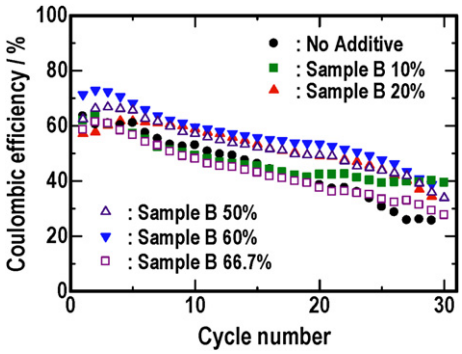

Fig. 4. Charge–discharge cycling tests results of lithium in EM + siloxane, SUS working electrode, Ips = 0.5 mA cm^{-2}, Qp = 0.50 mAh cm^{-2}, discharge cut-off voltage: 1.5 V vs. Li/Li^+.

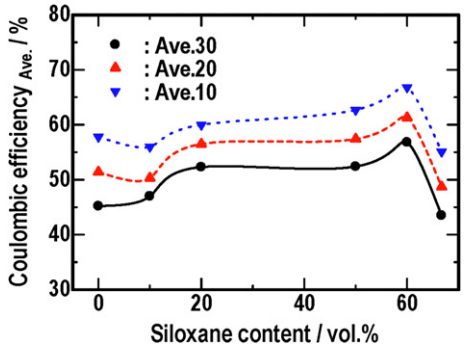

Fig. 5. Relationship between siloxane content and average lithium cycling efficiency (Coulombic efficiency $_{Av.}$), EM + siloxane, SUS working electrode, Ips = 0.5 mA cm^{-2}, Qp = 0.50 mAh cm^{-2}, discharge cut-off voltage: 1.5 V vs. Li/Li$^+$.

diffusion processes are important factors as rate-determining steps for electrode reaction. AC impedance measurements were carried out by using Li/SUS coin cells to investigate lithium/electrolyte interface in EM + siloxane in more detail. Li is deposited on SUS before impedance measurements. So, impedance measurements were carried out for the Li/Li cells.

Fig. 6 shows Cole–Cole plot of Li/Li (on SUS) cells in 1 M $LiPF_6$-EM with and without siloxanes. Impedance measurements were carried out after end of third charge (plating Li on SUS). A point of intersection (R_1) between x-axis and semi-circle at high AC frequency region corresponds to electrolyte conductivity. Electrolyte conductivities of EM + siloxanes become larger with an increase in amounts of siloxanes than EM alone being due to an increase in viscosity as already explained in the Section 3.1. Diameters of semi-circle ($R_2 - R_1$) correspond to interfacial resistance. After third charge, impedance values of the electrolyte/Li interface in EM + siloxanes were smaller than that in EM alone. These results suggest that impedance of the surface layer of lithium in EM + siloxane is thinner than that in EM alone. Electrode/electrolyte interface in EM + siloxane is physically and/or chemically different from that in EM alone.

3.4. Morphology of electrochemically deposited lithium

Li/SUS coin cells were disassembled after charging. Visual observation was carried out for these cells to investigate morphology of electrochemically deposited lithium (Fig. 7). In EM alone, deposition of lithium is not uniform over working electrode

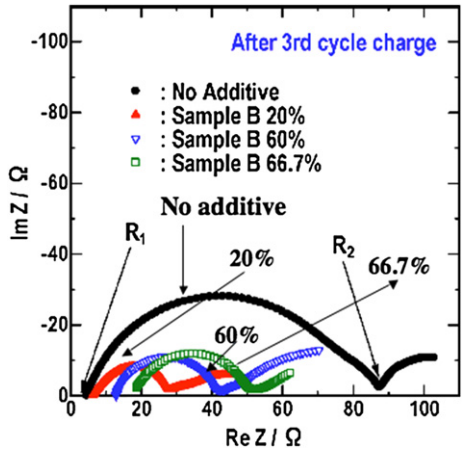

Fig. 6. Cole–Cole plot of Li/electrolyte interface, Li/Li cells, EM + sample B after third charge, Ips = 0.5 mA cm^{-2}, Qp = 0.50 mAh cm^{-2}, discharge cut-off voltage: 1.5 V vs. Li/Li$^+$.

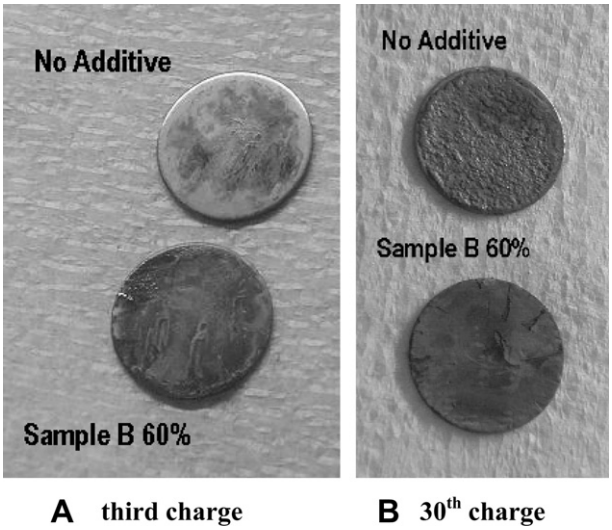

Fig. 7. Photographs of morphology of lithium deposition in EM with and without siloxane (sample B), A) third charge, B) 30th charge, SUS working electrode, Ips = 0.5 mA cm^{-2}, Qp = 0.50 mAh cm^{-2}, discharge cut-off voltage: 1.5 V vs. Li/Li$^+$.

surface. Morphology of deposited lithium becomes rougher with an increase in cycle number. By mixing siloxane, lithium deposition is more uniform and smoother than EM alone. So, mixing siloxane is effective on both smooth lithium deposition and suppressing the electrolyte reduction.

3.5. Model for interface between lithium electrode and electrolyte solutions

Summarizing the results of lithium cycling efficiency measurements, impedance measurements and morphology of lithium deposition, the following mechanism may be proposed for the improvement of lithium cycling efficiency by addition of siloxane. This mechanism is the same as reported in the previous work [10]. Fig. 8 shows the proposed models for cycling efficiency enhancement by adding siloxane (please see Fig. 5 as well). Just after charging (lithium deposition), freshly deposited lithium is chemically active. On the lithium surface, EM is chemically reduced by lithium and produces the surface film. Reduction products were reported to be solid compounds and gas compounds [18,20]. Solid compounds remained on the lithium produce SEI. Fig. 8(a): By no addition of siloxane, surface film is composed of reduction products of EM. Fig. 8(b): By small addition of siloxane, surface film is mainly composed of reduction products of EM. Small amounts of siloxane is involved in SEI or it adsorbs on SEI surface. Siloxane is less reactive than EM. Fig. 8(c): By medium amounts of siloxane (60 vol.% sample B), the surface film is thin and is composed of both the reduction product of EM and siloxane. Fig. 8(d): By adding larger amounts of siloxane, excess and thick siloxane layer exists around lithium electrode. This excess siloxane may be resistive for smooth charge–discharge of lithium (lithium ion diffusion). Then, lithium cycling efficiency improves by adding siloxane and shows the maximum value against addition amounts of siloxane.

3.6. Chemical composition of SEI on anodes

FT-IR spectroscopy was carried out to investigate chemical composition of SEI on anode surface in EM + siloxane. IR samples were prepared as follows. Two Li/natural graphite coin cells were fabricated. Two cells contained electrolyte solution of 1 M $LiPF_6$-EC/EMC (3:7 in volume ratio) with and without siloxane, respectively. Both cells were cycled three times at constant current density of

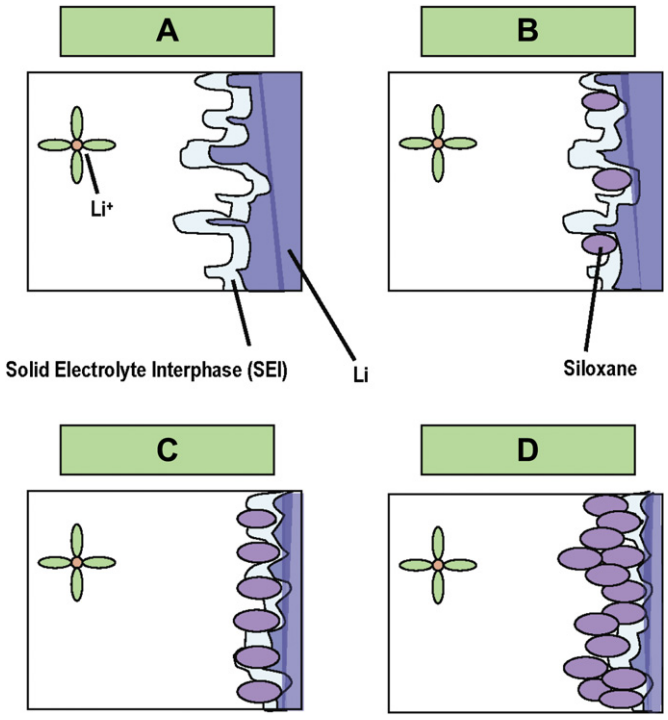

Fig. 8. Proposed mechanism for change in lithium cycling efficiency in EM + siloxane.

0.5 mA cm^{-2} and charge–discharge cutoff voltages of 1.5 V and 0.005 V. Cells exhibited 316 mAh g^{-1} on natural graphite weight at third cycle. This capacity corresponds to $C_6Li_{0.85}$. Cells were disassembled in argon gas filled drybox after de-intercalation of lithium ions from carbon anodes. Solid compounds (SEI) were observed on graphite electrodes of both cells. These graphite anodes were washed with EC/EMC (3:7 in volume ratio) solvents and dried in vacuum for 10 min at 25 °C. IR analyzed SEI films of these graphite anodes. There are several reasons why C_6Li_x is used instead of lithium metal in IR measurements here. First reason is handling difficulty of porous and fragile lithium after cycling. Second reason is that discussion is more comprehensive for carbon since data reported on chemical composition of SEI film of carbon surface is much more than those of lithium metals. Chemical composition of SEI of C_6Li_x is reported to be the same as that of lithium metal since the SEI is formed by reduction of electrolyte solutions by lithium [18]. SEI is composed of many organic and inorganic compounds [18,20]. Typical compounds are lithium alkyl carbonates (RCO_2OLi), $(CH_2OCO_2Li)_2$ and Li_2CO_3 for cyclic carbonates such as EC. SEI in linear cycling carbonates such as EMC contains similar compounds of lithium alkoxide (ROLi), RCO_2OLi, $(CH_2OCO_2Li)_2$ and Li_2CO_3. Typical reactions between Li and electrolyte solutions are shown in equations Eqs.(1)–(5). There are several ways of production process of Li_2CO_3 [18,20]. For instance, Li_2CO_3 is produced from decomposition of $(CH_2OCO_2Li)_2$ (Eq. (2)) [20]. According to Eqs. (1) and (3), organic components $(CH_2OCO_2Li)_2$ form first on surface of electrodes and gradually changes to inorganic components (Li_2CO_3) with an increase in standing or charging time. As a result, organic components exist on surface of SEI and inorganic components exist inside SEI (near electrodes) as reported by study on chemical analysis in depth direction of SEI [20]. When reduction of electrolyte solutions by lithium is large, large amounts of organic components may be detected in SEI.

Fig. 9 shows IR spectroscopy results. Both SEI films prepared with and without siloxane show IR peaks exhibiting $ROCO_2Li$ or $(ROCO_2Li)_2$ and Li_2CO_3. $ROCO_2Li$ or $(ROCO_2Li)_2$ shows IR peaks

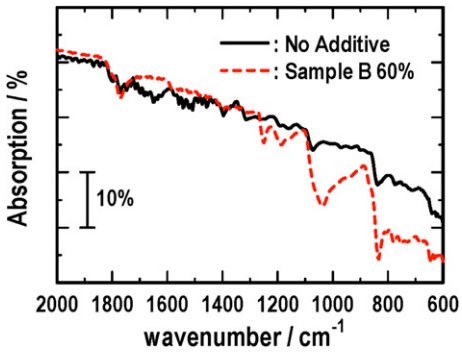

Fig. 9. FT-IR spectroscopy of graphite surface of Li/graphite cells after three cycles, EM with and without siloxane (sample B 60%), charge–discharge current density: 0.5 mA cm^{-2}, charge–discharge cutoff voltages of 1.5 V and 0.005 V.

around 1630–1690 cm^{-1}, 1300–1350 cm^{-1} and 1400 cm^{-1} [20]. Separation of these peaks for two compounds is almost impossible. Li_2CO_3 shows IR peaks around 1504 cm^{-1}, 1428–1430 cm^{-1} and 870 cm^{-1} [20]. 1750–1800 cm^{-1} corresponds to C=O vibration. It may correspond to $ROCO_2Li$ or $(ROCO_2Li)_2$. However, it is hard to identify this peak. IR spectra of SEI with siloxane show SiOR and SiOSi around 1050 cm^{-1}. These spectra are the same as that of siloxane as used for electrolyte preparation. From IR spectroscopy, following results are obtained. First, main chemical components of SEI are produced from reduction of EC/EMC by lithium both for with and without siloxane. Second, SEI with siloxane contains more inorganic compounds (Li_2CO_3) and less organic compounds of $ROCO_2Li$ or $(ROCO_2Li)_2$ than those of electrolyte solution without siloxane. Third, SEI with siloxane shows siloxane peaks even after washing with EC/EMC. Siloxane still remains in SEI without reduction or oxidation even after cycles. These results suggest that siloxane is captured in solid SEI and this special SEI structure may suppress excess reaction of electrolyte solutions by lithium. These results agree to the interfacial model proposed in Fig. 8.

$$2EC + 2Li \rightarrow (CH_2OCO_2Li)_2 + C_2H_4 \quad (1)$$

$$(CH_2OCO_2Li)_2 \rightarrow Li_2CO_3 + C_2H_4 + CO_2 + 1/2O_2 \quad (2)$$

$$2EMC + 2Li \rightarrow LiOC_2H_5 + LiOCO_2CH_3 + CO \quad (3)$$

$$2EMC + 2Li \rightarrow LiOCO_2C_2H_5 + LiOCH_3 + CO \quad (4)$$

$$EMC + 2Li \rightarrow Li_2CO_3 + 3/2C_2H_6 \quad (5)$$

3.7. Thermal stability tests of electrolyte solutions with and without siloxane

DSC measurements were carried out to investigate the reaction behavior of electrolyte solutions and lithium. In these measurements, instead of lithium metal, graphite–lithium (C_6Li_x) was used [10].

Fig. 10 shows the DSC results for C_6Li_x with electrolytes. C_6Li_x was prepared by charge–discharge of Li/graphite coin cells. Charge–discharge cycling was carried out twice between 0.005 V and 1.5 V at 0.5 mA cm^{-2}. Chemical composition of obtained product is $C_6Li_{0.85}$.

In case of $C_6Li_{0.85}$ with EM alone, two heat generation regions were observed. The first heat output was mild and started at 130 °C. It continued until a sharp exothermic peak appeared around 300 °C. A possible mechanism for these DSC results is as follows [21]. First mild heat output corresponds to the reduction of EM by lithium

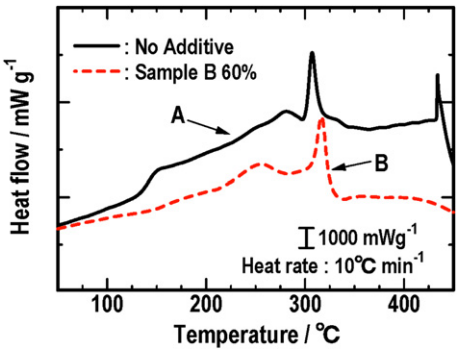

Fig. 10. DSC results of $C_6Li_{0.85}$ + EM with and without siloxane (sample B), DSC curve A: EM (no additive) and DSC curve B: EM + sample B (60%).

inside graphite. This reaction has already occurred in first charge at room temperature and produced SEI film on graphite surface. At 130 °C, the PVDF, electrode binder, swells. Then, the carbon that is not covered with SEI appears, and lithium inside carbon reacts with electrolyte solution [21]. SEI is consisted of several chemical materials. Another possibility as the cause for first heat output is suggested to be the decomposition of part of SEI compounds [22] or the conversion of metastable SEI components to stable SEI components [23]. At 300 °C, the surface SEI film is broken. Almost the whole of carbon surface appears, and lithium remained in graphite reacts vigorously with electrolyte solution [21].

In case of $C_6Li_{0.85}$ with the EM + siloxane, two small heat outputs were observed at 130 °C–250 °C and 315 °C. These heat outputs are similar to those of $C_6Li_{0.85}$ with EM alone. These heat output mechanism may be the same as in case of $C_6Li_{0.85}$ with EM alone. Starting temperatures of heat outputs using EM with siloxane were a little bit higher than those of EM alone. Total heat amount based on lithium weight between 120 and 350 °C of $C_6Li_{0.85}$ with siloxane (1.52 kJ g^{-1}) is a little bit smaller than those of EM alone (1.75 kJ g^{-1}). This small difference arises from the physical properties of SEI such as compactness and thickness. Addition of carbonate-modified siloxane exhibited small effects on the improvement of thermal stability of C_6Li_x anodes. These results may be due to the phenomenon that a part of liquid state siloxanes fluids from SEI film capturing siloxane with an increase in temperature.

3.8. Charge–discharge cycling properties of lithium in Si–C and Fe_2O_3 anodes in the electrolyte solutions with siloxanes

Effect of mixing siloxane on cycling efficiency of lithium metal was obtained as explained above. Effects of siloxane on other anode materials than lithium metal were briefly examined in this work. As another anode materials, Si–SiO_2–carbon composite (Si–C) and α-Fe_2O_3 were used. These anode materials have different reaction mechanism with Li from that of lithium metal. Charge–discharge reaction of lithium metal is electrochemical plating of lithium and stripping of Li^+ ions. However, these anode materials are charged to close to 0 V vs. Li/Li+. So, as in case of lithium metal, suppression of electrolyte reduction by lithium is necessary to improve charge–discharge cycling efficiencies.

3.8.1. α-Fe_2O_3 anodes

Influence of siloxane on charge–discharge cycling performance of α-Fe_2O_3 was examined. Reaction between Li and α-Fe_2O_3 proceeds by conversion reaction mechanism (eq. (6)) [15]. α-Fe_2O_3 shows capacity of 1007 mAh g^{-1} based on α-Fe_2O_3 weight according to 6Li/α-Fe_2O_3 reaction.

$$6Li + \alpha - Fe_2O_3 \rightarrow 2Fe + 3Li_2O \quad (6)$$

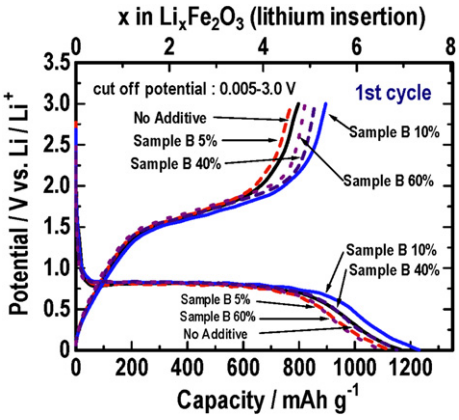

Fig. 11. Charge–discharge voltage curves of Li/α-Fe_2O_3 cells, EM with and without siloxane (sample B), Ips = 0.5 mA cm^{-2}, charge–discharge cut-off voltages: 0.005 and 3.0 V.

Fig. 11 shows charge–discharge voltage profiles of Li/α-Fe_2O_3 coin cells with EM + siloxanes (sample B: 5, 10, 40 and 60 vol.% and no additive). Fig. 12 shows the relation between discharge capacity and cycle number of Li/α-Fe_2O_3 cells with EM + siloxanes. Discharge capacity density (mAh g^{-1}) in *y*-axis of Fig. 12 is calculated based on α-Fe_2O_3 active material weight put in the coin cells. Discharge means discharging Li^+ ions from (Fe + Li_2O) electrodes. Both discharge capacity density and degradation of discharge capacity with an increase in cycle number of Li/α-Fe_2O_3 cells depend on siloxane content in EM + siloxanes. At 15th cycle, discharge capacity and degree of suppression of degradation of discharge capacity is better in the order of sample B 10% > 40% > no additive > 5% > 60%. In case of α-Fe_2O_3, 10% or 40% sample B exhibited better cycling performance than that of EM alone. Small amounts of sample B 5% and large amount of sample B 60% show worse cycling performance than that of EM alone. In case of lithium metal, 60% sample B showed the best cycling performance. So, optimum-mixing amount of siloxane for enhancement of cycling performance must be different and individually checked for each anode material.

3.8.2. Si–C anodes

Charge–discharge reaction of Si–C (Si–SiO_2–carbon composite) is electrochemical alloying between Li and Si in SiO_2 matrix and discharging Li^+ ions from Li–Si alloys. At first charge of Li/Si–C cell, Li–Si alloy and Li–Si–O compounds form (eq. (7)). Following charge–discharge cycles, reversible reaction proceeds as shown in

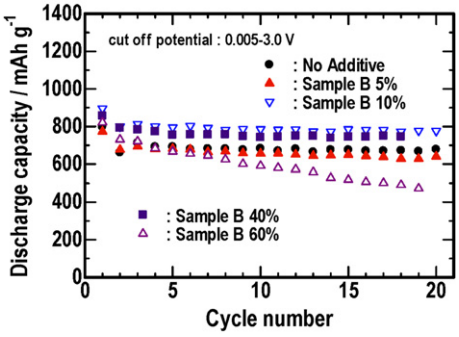

Fig. 12. Charge–discharge cycling tests results of Li/α-Fe_2O_3 cells, EM with and without siloxane (sample B), 0.2 mA cm^{-2} except for first cycle (0.5 mA cm^{-2}), charge–discharge cut-off voltages: 0.005 and 3.0 V.

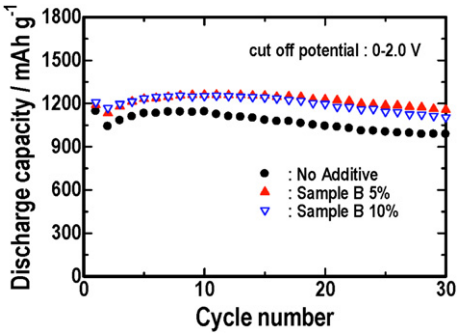

Fig. 13. Charge–discharge cycling tests results of Li/Si–C cells, EM with and without siloxane (sample B), 0.2 mA cm^{-2} except for first cycle (0.5 mA cm^{-2}), charge–discharge cut-off voltages: 0 and 2.0 V.

eq. (8) since Li–Si–O compounds were electrochemically irreversible. Si–C anode shows cycling capacity of 2200 mAh g^{-1} based on Si–C weight when SiO_2: Si is 1:1 in weight ratio with neglecting weight of carbon surface film and calculating irreversible formation of Li–Si–O compounds.

$$(SiO_2 + Si) + 7.91\ Li \rightarrow 1.42\ Li_{4.4}Si + 1/3Li_2SiO_3 + 1/4Li_2SiO_4 \quad (7)$$

$$Si + 4.4Li \rightarrow Li_{4.4}Si \quad (8)$$

Fig. 13 shows the charge–discharge cycling test results of Li/Si–C cells in EM + siloxanes (sample B: 5 and 10 vol.%; and no additive). Discharge capacity density (mAh g^{-1}) in *y*-axis of Fig. 13 is calculated based on the Si–C active material weight put in coin cells. Discharge means discharging Li^+ ions from Li–Si alloys in Si–C electrodes. Both discharge capacity densities and cycle life in EM + siloxanes were better than those in EM alone. In case of Si–C anodes, 5 vol.% siloxane showed better discharge capacities than 10 vol.% siloxane.

4. Conclusion

Charge–discharge cycling efficiencies of lithium metal were improved by mixing carbonate-modified siloxane (4-(2-bis (trimethylsilyloxy)methylsilylethyl)-1,3-dioxolan-2-one) into 1 M $LiPF_6$-EC/EMC. The impedance of anode/electrolyte interface decreased by mixing siloxanes. Mechanism of enhancement of lithium cycling efficiency is considered to be due to the suppression of excess reduction of $LiPF_6$-EC/EMC by lithium and growth of surface film (SEI) on lithium. Infrared study indicates SEI formed by siloxane mixing electrolyte contains siloxane and more inorganic compounds than those by $LiPF_6$-EC/EMC alone. Better cycling behavior of Si–C and α-Fe_2O_3 anodes is obtained by mixing siloxane as well. Heat-output of graphite-lithium anodes with 1 M $LiPF_6$-EC/MEC electrolyte solutions tends to decrease by mixing siloxane. By modifying chemical structure of siloxanes, we expect to obtain the more improvement of charge–discharge cycling performance and thermal stability of rechargeable cells with various lithium-based anode materials.

References

[1] N. Tamura, R. Ohshita, M. Fujimoto, M. Kamino, S. Fujitani, J. Electrochem. Soc. 150 (2003) A679.
[2] L.A. Dominey, in: G. Pistoia (Ed.), Lithium Batteries, Elsevier, The Netherlands, 1994 (Chapter 4).
[3] R. McMillan, H. Slegr, Z.X. Shu, W. Wang, J. Power Sources 81–82 (1999) 20.
[4] J. Yamaki, I. Yamazaki, M. Egashira, S. Okada, J. Power Sources 102 (2001) 288.
[5] M. Ihara, B.T. hang, K. Sato, M. Egashira, S. Okada, J. Yamaki, J. Electrochem. Soc. 150 (2009) A1476.
[6] M. Ue, Extended Abstracts of the Battery and Fuel Cell Materials Symposium. Gratz, Austria, p. 53 (2004).
[7] K. Amine, Q. Wang, D.R. Vissers, Z. Zhang, N.A.A. Rosii, R. West, Electrochem. Commun. 6 (2006) 429.
[8] X.J. Wang, H.S. Lee, H. Li, X.Q. Wang, X.J. Huang, Electrochem. Commun. 12 (2010) 386.
[9] T. Inouse, S. Tada, H. Morimoto, S. Tobishima, J. Power Sources 161 (2006) 550.
[10] T. Takeuchi, S. Noguchi, H. Morimoto, S. Tobishima, J. Power Sources 195 (2010) 580.
[11] M. Mori, Y. Narukawa, K. Naoi, D. Futeux, J. Electrochem. Soc. 145 (1998) 2340.
[12] M. Miyachi, H. Yamamoto, H. Kawai, T. Ohta, M. Shirakawa, Extended Abstracts of 206th Electrochemical Society Meeting, Abs. No. 311, 2004.
[13] T. Morita, N. Takami, Extended Abstracts of 206th Electrochemical Society Meeting, Abs. No. 312, 2004.
[14] Jpn. Kokai Tokkyo Koho (Jpn. Patent application), JP2004–47404A, 2004.
[15] H. Morimoto, H. Watanabe, S. Tobishima, Electrochemistry 78 (2010) 339.
[16] M. Ue, J. Electrochem. Soc. 141 (1994) 3336.
[17] W. Biltz, W. Fischer, Z. Phys. Chem. (Leipzig) 151A (1930) 12.
[18] D. Aurbach, E. Granot, Electrochim. Acta 42 (1997) 697.
[19] E. Peled, D. Golodnitsky, J. Pencier, in: J.O. Besenhard (Ed.), Handbook of Battery Materials, Wiley-VCH, Germany, 1999 (Chapter 6).
[20] M. Lu, H. Cheng, Y. Yang, Electrochim. Acta 53 (2008) 3539.
[21] J. Yamaki, H. Takatsuji, T. Kawamura, M. Egashira, Solid State Ionics 148 (2002) 241.
[22] A. Du Pasquier, F. Disma, T. Bowmer, A.S. Gozdz, G. Amatucci, J.M. Tarascon, J. Electrochem. Soc. 145 (1998) 472.
[23] M.N. Richard, J.R. Dahn, J. Electrochem. Soc. 146 (1999) 2068.